Dielectric Relaxation of Styrene–Isoprene Diblock Copolymer Solutions: A Selective Solvent System

Ming-Long Yao, Hiroshi Watanabe, Keiichiro Adachi, and Tadao Kotaka*

Department of Macromolecular Science, Faculty of Science, Osaka University, Toyonaka, Osaka 560, Japan

Received March 21, 1991; Revised Manuscript Received July 12, 1991

ABSTRACT: Dielectric measurements were made on solutions of styrene–isoprene (SI) diblock copolymers in an I-selective solvent, *n*-tetradecane (C14), in which the S-blocks formed a rigid phase and the I-blocks were swollen. The solutions exhibited dielectric normal-mode relaxation due to the fluctuation of the end-to-end vector of the I-blocks having dipoles aligned in the same direction parallel along their contour and being tightly anchored on the rigid S-phase. The nominal relaxation time τ_n (evaluated as the reciprocal of the loss maximum frequency ω_{max}) became shorter and the relaxation mode distribution, narrower, as C14 was added to decrease SI concentration c_{SI}. These results were attributable to a decrease in spatial and thermodynamic confinements for the tethered I-blocks. However, even for dilute solutions in which the SI micelles were randomly dispersed, the mode distribution was still considerably broader than that of homo-PI systems, reflecting a situation in that the tethered I-blocks were still densely populated, and thus subjected to strong thermodynamic confinement in the I-corona phase. For the solutions with intermediate c_{SI}, we found a new dielectric relaxation slower than the normal mode of the I-blocks. This new relaxation mode was found also in C14 solutions of styrene–butadiene (SB) diblock copolymer and should not be due to type-A dipoles of the I-blocks. Rheological measurements revealed that these SI/C14 and SB/C14 solutions exhibited prominent plasticity characteristic of an ordered array of the micelles (a macrolattice). The new mode can thus be related to a stable macrolattice formed in these solutions.

I. Introduction

In a previous paper[1] we discussed the dielectric behavior of polystyrene (PS)–*cis*-polyisoprene (PI) diblock copolymers (SI) in the bulk state. In such systems under an ambient condition, styrene (S) blocks form glassy domains on which isoprene (I) blocks are tightly bound to form a rather densely populated, tethered rubbery-chain phase. The features of such a microdomain structure[2] are related to two kinds of confinements imposed on the blocks:[3–6] the spatial confinement that prohibits a block chain to cross the domain boundary, and the thermodynamic confinement that forces the configuration of block chains belonging to the same domain to be coupled so that the segment density profile is kept uniform throughout to the extent allowed by the (bulk and/or osmotic) compressibility in the domains. Such confinements should also exert strong influence especially on the dynamics of the tethered I-block chains.

The PI chains have type-A dipoles aligned in the same direction parallel along the chain contour and exhibit so-called *dielectric normal-mode relaxation* due to the fluctuation of their end-to-end vectors.[7–10] Thus the SI diblock copolymer is a good model system for studying the dynamics of I-blocks tethered on the S-phase through dielectric spectroscopy. In bulk SI systems, the glass transition temperatures T_g^{PI} ($\simeq$200 K)[11] and T_g^{PS} ($\simeq$373 K)[11] of PI and PS blocks are widely separated. Measurements were conducted at temperatures between T_g^{PI} and T_g^{PS} so that we were able to examine the dynamics of the I-block chains tethered on the rigid S-domains and confined in the I-phase.

In the previous study[1] we found that the shape of the dielectric loss ϵ'' curve that reflects the dielectric relaxation mode distribution is much broader for the tethered I-block chains than that for bulk homo-PI chains. The longest relaxation time is quite likely much longer for the former than for the latter.

The confinements mentioned above and thus motion of the I-blocks in the microphase-separated SI systems should change upon dilution with an I-selective solvent, for example, *n*-tetradecane (C14). The solvent C14 dissolves I-blocks but hardly swells the glassy S-domains so that the S–I junctions in SI/C14 solutions have a negligibly small mobility as in the case of bulk SI. The spatial confinement becomes weakened by dilution with increasing domain size (relative to the dimension of the I-blocks in the confinement free state). Thermodynamic confinement also becomes weakened, because the compressibility in the I domains increases. Thus it is of interest to examine the effects of addition of C14 to SI diblock copolymer systems. The effects of the changes in the two confinements on the global motion of the tethered I-block chains should be most clearly observed on SI/C14 systems.

From the above point of view, we examined the dielectric behavior of SI/C14 systems. This paper presents the results. On interpreting the results, we also utilize the rheology–structure relationship for SB/C14 solutions[12–18] similar to the present SI/C14 systems.

II. Experimental Section

Materials: Polystyrene–*cis*-polyisoprene (SI) and polystyrene–polybutadiene (SB) diblock copolymers were prepared via anionic polymerization according to our laboratory routine.[1] Three SI and their precursor PI samples were used. An SB sample was also used for comparison. The samples were characterized by combined light scattering–gel permeation chromatography. The details were described elsewhere.[1] Table I summarizes their characteristics. The code numbers indicate the weight-average molecular weights M_W of the constituent blocks in units of 1000. Commercial *n*-tetradecane (C14) was used as received (Tokyo Kasei Co., guaranteed grade) without further purification.

Measurements: Dielectric measurements were made with a capacitance cell and a transformer bridge (GR 1615A; General Radio) described previously.[1,10] The measurements were conducted mostly at 30 °C on solutions of SI, SB, and PI samples in C14 with various concentrations. The temperature–frequency superposition was not attempted here to avoid complication due to structural changes induced by heat. Instead, to obtain information on the microdomain structure and its possible changes, we conducted rheological measurements with a laboratory rheometer (IR-200; Iwamoto Seisakusho) most extensively on a 30 wt % solution of SI(12.5–9.5) in C14 at various tem-

0024-9297/91/2224-6175$02.50/0 © 1991 American Chemical Society

Table I
Characteristics of Polymer Samples

code	$10^{-3}M_w$	M_w/M_n	S content, wt %
	SI Diblock Copolymer[a]		
SI(12.5–9.5)	22.0	1.06	55.2
SI(42–42)	84.0	1.06	49.4
SI(43–86)	129.0	1.06	33.3
	SB Diblock Copolymer[b]		
SB(8.6–8.5)	17.1	1.08	50.5
	PI Precursor[a]		
PI(9.5)	9.5	1.06	
PI(42)	42.0	1.06	
PI(86)	86.0	1.06	

[a] cis:trans:vinyl ≅ 75:20:5 for I. [b] cis:trans:vinyl ≅ 40:50:10 for B.

peratures. The data were interpreted on the basis of the rheology–structure relationship established through previous rheological and small-angle X-ray scattering (SAXS) studies on SB diblock copolymer solutions in selective solvents including C14.[12-18]

The solutions subjected to dielectric and rheological measurements were prepared in the following way. Prescribed amounts of a polymer sample and the nonvolatile solvent C14 were mixed with excess benzene to make an about 5% homogeneous solution. Benzene was then allowed to evaporate completely. The solution was annealed at 60–90 °C for 15–30 min in the capacitance cell or the rheometer assembly to achieve equilibrium morphology just before the measurements.[12]

To obtain some idea on the rigidity of S-domains that is related to the mobility of the S–I junction points in SI/C14 solution, we determined with a differential scanning calorimeter (DSC 20; Seiko I&E Co.) the glass transition temperature T_g^{PS} of PS swollen in C14. Compression-molded PS films of thickness ≅0.5 mm were immersed in C14 for 10 days at room temperature (≅20 °C) and further at 70 °C for 1 h. The swollen films were then taken out, weighed to determine the swelling ratio, and subjected to DSC with a heating rate of 10 °C/min.

The T_g^{PS} and swelling ratio of the films were found, respectively, to be 59 ± 5 °C and 10 ± 1 wt % for PS of $M_{PS} = 10.5 \times 10^3$ and 93 ± 3 °C and 2 ± 0.5 wt % for PS of $M_{PS} = 46.4 \times 10^3$. In the present SI/C14 solutions involving S-blocks with M_S of $43 \times 10^3 \geq M_S \geq 12.5 \times 10^3$ (cf. Table I), the T_g^S of the S-phase are between these two values and thus the mobility of S–I junctions should be negligibly small at the temperatures <60 °C where most of the measurements were carried out.

III. Molecular Motion and Dielectric Normal-Mode Relaxation

As shown in the previous work on bulk SI,[1] the dielectric loss ϵ'' for the normal-mode relaxation can be described by eq 1 not only for homo-PI chains (regardless of being entangled or unentangled)[8-10] but also for I-blocks in an SI copolymer under the spatial and thermodynamic confinements.

$$\epsilon'' = -\Delta\epsilon \int_0^\infty \frac{d\Phi(t)}{dt} \sin 2\pi f t \, dt \quad \text{(for normal-mode relaxation)} \quad (1)$$

Here f is the frequency, and $\Delta\epsilon$, the relaxation intensity. The autocorrelation function, $\Phi(t)$, is related to the end-to-end vector $\mathbf{R}(t)$ of the I-block at time t as

$$\Phi(t) = \frac{\langle \mathbf{R}(t)\cdot\mathbf{R}(0)\rangle}{\langle \mathbf{R}^2\rangle} = \sum_p g_p \exp[-t/\tau_p] \quad (2)$$

Here for convenience of the following explanation, we have formally decomposed the $\Phi(t)$ into the relaxation modes with the intensity factors g_p and characteristic times τ_p, with $p = 1$ representing the slowest relaxation mode. From

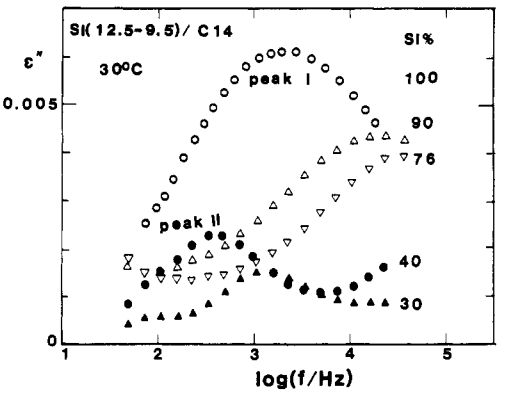

Figure 1. Frequency dependence of dielectric loss ϵ'' at 30 °C for SI(12.5–9.5)/C14 solutions with various concentrations as indicated.

eqs 1 and 2, we can write ϵ'' in terms of g_p and τ_p as

$$\epsilon'' = \Delta\epsilon \sum_p g_p \frac{\omega\tau_p}{1+\omega^2\tau_p^2}, \quad \omega = 2\pi f \quad (3)$$

For monodisperse linear homo-PI chains, the slowest mode ($p = 1$) has the largest intensity and dominates the dielectric relaxation.[10] Correspondingly they exhibit a sharp ϵ'' peak practically of the same shape. In fact, the behavior of these chains are semiquantitatively described by the Rouse and/or tube models that predict $g_1 \gg g_p$ for $p > 1$:[10,19]

$$g_p = 8/(\pi^2 p^2) \quad \text{and} \quad \tau_p = \tau_1/p^2; \quad p = 1, 3, 5, \ldots \quad (4)$$

Thus the dielectric relaxation time τ_n that is defined from the loss maximum frequency f_m by

$$\tau_n = 1/2\pi f_m \quad (5)$$

is close to the longest relaxation time τ_1. However, this is not at all the case for the tethered I-block chains.[1]

As can be seen from eq 3, the shape of the ϵ'' curve for the normal-mode relaxation reflects the mode distribution of $\Phi(t)$ (distribution of g_p and τ_p): The broader the distribution, the broader the ϵ'' curves. As is quite common for all types of relaxation phenomena, the dependence $\epsilon'' \propto f$ is observed only at time scales longer than the longest relaxation time τ_1, or, equivalently, only at sufficiently low frequencies $f < 1/2\pi\tau_1$ (cf. eq 3). At higher f ($>1/2\pi\tau_1$), the ϵ'' is generally dependent on f more weakly. These features enable us to discuss the relaxation mode distribution of the end-to-end vector fluctuation of the I-blocks from the shape of the ϵ'' curves.

IV. Results and Discussion

IV-1. Overview: Figure 1 shows frequency (f) dependence of the dielectric loss factors ϵ'' at 30 °C for C14 solutions of SI(12.5–9.5) with SI concentrations $100 \geq c_{SI}$ (wt %) ≥ 30. Prominent plasticity was found for all the systems (even at c_{SI} as low as 30 wt %), suggesting that the microdomains in the solutions were arranged on a regular lattice referred to as a macrolattice.[12-18]

As seen in Figure 1, two different types of loss peaks are found in our experimental window. For $c_{SI} \geq 76$ wt %, a peak appears at $f \geq 2000$ Hz. This peak, referred to as the peak I, rapidly shifts with decreasing c_{SI} toward a much higher f side and finally becomes out of sight for $c_{SI} < 76$ wt %. For $c_{SI} \leq 40$ wt %, another peak, referred to as the peak II, emerges at low $f < 2000$ Hz. With further decreasing c_{SI}, the peak II also shifts rapidly to the high f side.

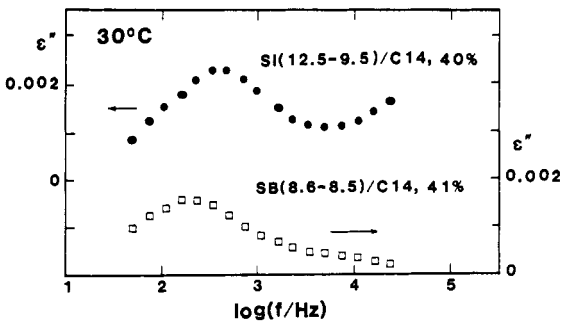

Figure 2. Comparison of dielectric loss curves of SI(12.5–9.5)/C14 (40 wt %) and SB(8.6–8.5)/C14 (41 wt %) solutions at 30 °C.

Since C14 is a nonsolvent toward S-blocks but a good solvent toward I-blocks, the S-blocks form precipitated rigid domains, and the I-blocks, cilia with tightly anchored ends, i.e., tethered chains. The two peaks found in Figure 1 are not due to the segmental modes of the S- and I-blocks that are too slow and too rapid, respectively, to be observed for the SI/C14 solutions at the temperatures and frequencies examined.

To clarify the origin of the two peaks, we carried out dielectric measurements on C14 solutions of SB(8.6–8.5) at 30 °C. The molecular characteristics, e.g., the degree of polymerization n and the characteristic ratio C_∞ of the diene blocks as well as the styrene content w_S, are nearly the same for SB(8.6–8.5) ($n = 157$, $C_\infty = 5.4$,[20] $w_S = 50.5\%$) and SI(12.5–9.5) ($n = 140$, $C_\infty = 5.3$,[20] and $w_S = 55.2\%$), the latter being examined in Figure 1. In addition, the solvent C14 is equally good for the B- and I-blocks, and their microdomain structures should be nearly the same for the C14 solutions of these SB and SI copolymers of the same c. Thus, in moderately concentrated to dilute C14 solutions where the local frictions of the I- and B-blocks are essentially determined by C14, the global motion of the diene blocks of the SB(8.6–8.5) and SI(12.5–9.5) copolymers should be essentially the same. However, differing from the I-block, the B-block has no type-A dipoles and exhibits no dielectric normal-mode relaxation. Thus, if a dielectric relaxation is observed only for the SI/C14 solution but not for the SB/C14 solution of the same c, it can be attributed to the type-A dipoles of the I-blocks (i.e., to the normal-mode relaxation). On the contrary, if a relaxation is observed for both solutions, the relaxation is not due to the type-A dipoles.

At high $c_{SB} > 60$ wt %, the SB(8.6–8.5)/C14 solution exhibited very small ϵ'' ($\lesssim 0.001$) and no peak was observed in our experimental window. This result enables us to assign the peak I found in Figure 1 for SI(12.5–9.5)/C14 of $c_{SI} \geq 76$ wt % to the dielectric normal-mode relaxation of the I-blocks, as concluded for bulk SI in the previous work.[1] However, at $c_{SB} \leq 41$ wt %, the SB/C14 solution also exhibited a dieletric peak, as shown in Figure 2. The peak locations are roughly the same for SI(12.5–9.5)/C14 and SB(8.6–8.5)/C14 of nearly the same c. Thus the peak II found for the former is not due to the type-A dipoles but to some other reason(s) common to the SI and SB solutions.

The trend similar to that found in Figure 1 was also seen for other SI/C14 solutions. Figure 3a shows the ϵ'' curves of SI(42–42)/C14 solutions with various c_{SI} at 30 °C, and for comparison Figure 3b shows those of the precursor PI(42)/C14 solutions. In Figure 3a, the ϵ'' peaks of the solutions with $c_{SI} \geq 50$ wt % are again attributable to the normal-mode relaxation, while the peak II is not observed at the frequencies examined here. For those

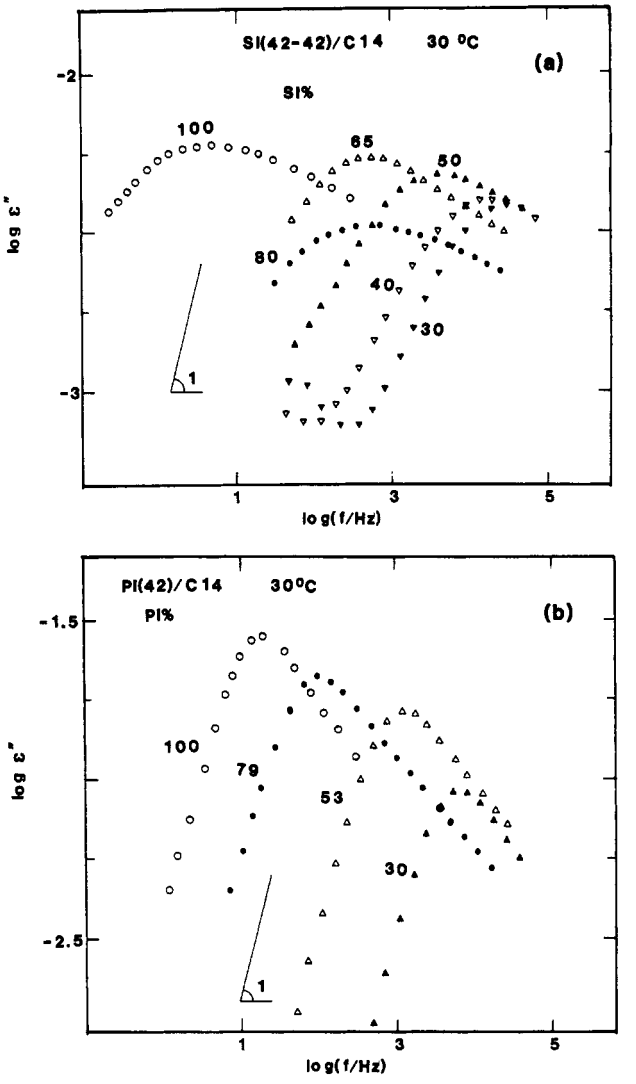

Figure 3. Frequency dependence of dielectric loss ϵ'' at 30 °C for (a) SI(42–42)/C14 and (b) PI(42)/C14 solutions with various concentrations as indicated. PI(42) is a precursor for SI(42–42). For SI(42–42) and PI(42) at bulk (c_{SI}, $c_{PI} = 100$ wt %), the time–temperature superposition held and the data at higher temperatures are reduced to 30 °C.

with $c_{SI} = 40$ and 30 wt %, however, we observe the normal-mode peak I relaxation at $f \gtrsim 10^4$ Hz and also note a tendency of increase of ϵ'' with decreasing $f < 300$ Hz that can be a sign of the peak II relaxation.

For C14 solutions of SI(43–86) having I-blocks longer than those of the two SI copolymers examined in Figures 1 and 3, we found the normal-mode relaxation peak I at 30 °C for $c_{SI} = 2$–20 wt %, as the results shown later in Figure 5.

IV-2. Normal-mode relaxation: We here discuss the feature of the normal-mode relxation. In Figure 3a, we see a striking feature that the ϵ'' peak height for SI(42–42)/C14 does not monotonously decrease with decreasing c_{SI}. Instead, it first decreases as c_{SI} decreases from 100 to 80 wt %, then increases with decreasing c_{SI} down to 65 wt %, and again decreases as c_{SI} further decreases below 65 wt %. This trend is found also for SI(12.5–9.5)/C14 solutions: As seen in Figure 1, the peak height of the solution with $c_{SI} = 90\%$ is considerably smaller than 90% of the height for the bulk system.

Because the ϵ'' curves of the SI/C14 systems are quite broad, as seen in Figures 3–5, and the terminal relaxation characterized by the relation $\epsilon'' \propto f$ (cf. eq 3) is not observed in our experimental window, the dielectric relaxation

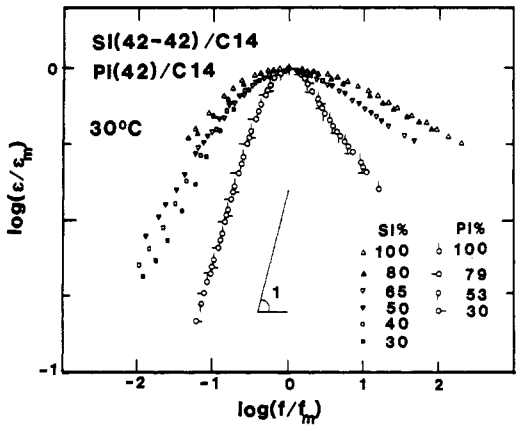

Figure 4. Comparison of ϵ'' curves reduced at peaks for SI(42–42)/C14 and PI(42)/C14 solutions at 30 °C. For the SI(42–42)/C14 solutions, the ϵ'' data for $f < 300$ Hz corresponding to the peak II relaxation (cf. Figure 1) are not shown.

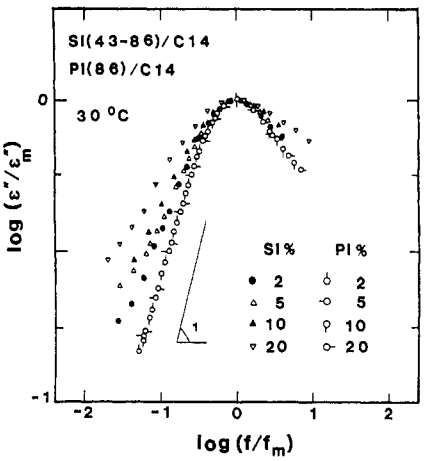

Figure 5. Comparison of ϵ'' curves reduced at peaks for SI(43–86)/C14 and PI(86)/C14 solutions at 30 °C.

intensity $\Delta\epsilon$ (cf. eq 1) cannot be accurately evaluated. Thus it is not certain whether $\Delta\epsilon$ changes nonmonotonously with c_{SI} as in the case of the ϵ'' peak height. However, the peculiar behavior of the peak height is enough to suggest some structural changes taking place in the SI/C14 systems.

One possibility for such a structural change is a change in the shape of the microdomains.[2,21] At 30 °C the S-domains hardley swell in the solvent C14, as suggested from the DSC results on PS films (see section II) and also from the results of a previous SAXS study on SB/C14 systems.[15] Thus the volume fraction ϕ_S of the S-phase decreases with decreasing c_{SI}. For c_{SI} = 80 and 65 wt % where an anomalous change in the peak height was found in Figure 3, the ϕ_S is estimated to be 35 and 27 vol %, respectively. These ϕ_S values are fairly close to the values for the transitions of the S-phase from lamellae to cylinders and from cylinders to spheres, respectively.[2,21] Such morphological transitions are characteristic of adding an I-selective solvent (C14) to SI copolymers with S/I composition ≅50/50 and may be related to the peculiar c_{SI} dependence of the peak height.

Apart from the peculiar behavior of the ϵ'' peak height, we see in parts a and b of Figure 3 a significant difference in the normal-mode relaxations for the C14 solutions of SI and homo-PI. The ϵ'' curves shift to the high f side for both solutions with decreasing c. However, the shape of the ϵ'' curves for SI solutions significantly changes with c, reflecting changes of the relaxation mode distribution, while that for the PI solutions does not change with c.

Figure 4 compares the shape of the ϵ'' curves (in the double-logarithmic scale) reduced at their peaks for the C14 solutions of SI(42–42) and its precursor PI(42). For the SI/C14 solutions with c_{SI} = 30 and 40 wt %, the data for $f < 300$ Hz are not included here so that the ϵ'' curves reflect only the feature of the normal-mode relaxation (cf. Figure 3a).

As seen in Figure 4, the shape of the ϵ'' curves and thus the dielectric mode distribution of PI(42)/C14 do not change even when c_{PI} is decreased from 100 to 30 wt %, as reported previously.[22] On the other hand, the mode distribution for SI(42–42) is quite broad for c_{SI} = 100 wt % (bulk) and becomes narrower and closer to that of PI(42)/C14 with decreasing c_{SI}. However, we still do not see through our experimental window the dependence, $\epsilon'' \propto f$, characteristic of the terminal relaxation behavior even for c_{SI} = 30 wt %.

Figure 5 compares similar reduced ϵ'' curves at 30 °C for SI(43–86)/C14 and corresponding PI(86)/C14 solutions of c_{SI} (or c_{PI}) between 20 and 2 wt %. For these SI/C14 solutions, the ϵ'' curve is already considerably narrow for c_{SI} = 20 wt % and becomes further narrower with decreasing c_{SI} down to 2 wt %.

In all SI/C14 solutions at 30 °C (cf. Figures 1–5), the I- and S-blocks should be strongly segregated, and the S-phase is in the glassy state as explained before. The S–I junctions have a negligibly small mobility which is hardly affected by the decrease of c_{SI} through dilution with C14. The major effects of dilution are thus to increase the volume fraction ϕ_I of the I-phase (containing I-blocks plus C14) and to decrease the I segment concentration c_{PI} in that phase. The decrease in c_{SI} and thus in c_{PI} tends to release the spatial constraint by providing more space to the I-blocks. The decrease in c_{PI} also increases the osmotic compressibility in the I-phase, which in turn releases the thermodynamic confinement on the I-blocks. Both of these effects allow the I-blocks at smaller c_{SI} to behave more like homo-PI chains with tethered ends. This explains qualitatively the results found in Figures 3–5 (apart from the peculiar c_{SI} dependence of the peak height seen in Figure 3a).

For SI(43–86)/C14 solutions with c_{SI} = 20–2 wt %, ϕ_S is estimated to be less than 5 vol % and thus spherical micelles with S-cores and I-corona should have been formed.[21] Rheological tests detected a structural transition upon dilution[12,16–18] of these solutions from c_{SI} = 20 to 2 wt %: The solution with $c_{SI} \geq 10$ wt % exhibited prominent plasticity at 30 °C and should possess a regular array (stable macrolattice) of the micelles.[12,16–18] The solution with c_{SI} = 5 wt % still exhibited plasticity but much less prominently as compared to those with $c_{SI} \geq 10$ wt %. Finally at c_{SI} = 2 wt %, the solution behaved just as a viscous liquid and exhibited no plasticity. Upon dilution of the solutions down to 2 wt %, thermodynamic interactions between the I-blocks belonging to different micelles become too weak to preserve a stable macrolattice. This explains the significantly narrow ϵ'' curve that reflects a narrow dielectric normal-mode distribution (cf. eq 3) for the 2 wt % SI/C14 solution examined in Figure 5. However, we still see a nonnegligible difference in the mode distribution between this solution and the PI(86) solutions.

In all SI(43–86)/C14 solutions with $20 \leq c_{SI}$(wt %) ≤ 2, the micelle size, i.e., the number of SI chains per micelle should be close to each other, as suggested from a previous SAXS study on an SB copolymer similar to SI(43–86) examined here.[15] This means that, even in a micelle in the solution with small c_{SI}, the I-corona chains tethered

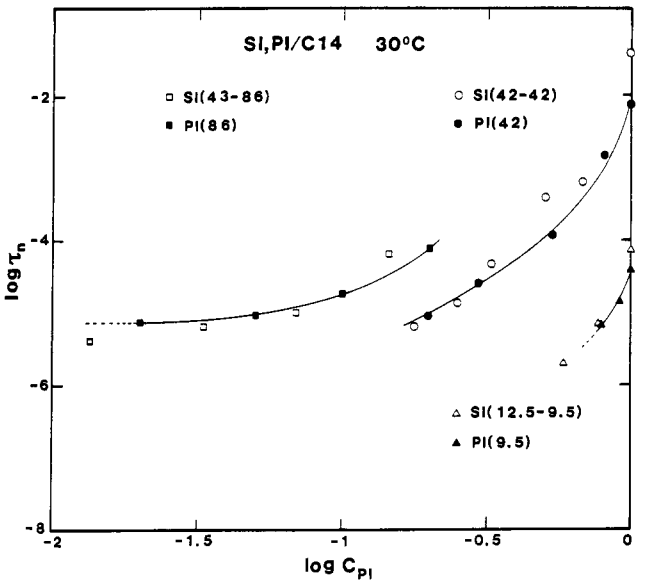

Figure 6. Comparison of dielectric relaxation times τ_n evaluated from the location of ϵ'' peaks for SI/C14 and PI/C14 solutions at 30 °C. Note that τ_n is close to the longest relaxation time τ_1 for the PI/C14 solutions, while $\tau_n \ll \tau_1$ for the SI/C14 colutions. For details, see text.

to the rigid S-core are still rather densely populated and thus are under strong mutual influence of the thermodynamic confinement to maintain the concentration profile acceptable in the I-corona phase. This difference in the environments of the I-chains is responsible to the difference in the mode distributions of the I-chains in SI/C14 and PI/C14 solutions found in Figure 5. A further study on this problem is now in progress.

IV-3. Normal-mode relaxation times: For SI/C14 and PI/C14 solutions, we evaluated the (nominal) dielectric relaxation time τ_n from the loss maximum frequency f_m using eq 5. Figure 6 compares dependences of τ_n at 30 °C on the I segment concentration c_{PI} for C14 solutions of SI and corresponding PI precursors. We see that the τ_n are longer for SI/C14 solutions (unfilled symbols) than for PI/C14 solutions (filled symbols) at high c_{PI} but opposite at low c_{PI}. However, we have to hasten to add that this result does not necessarily mean the I-blocks move more rapidly at low c_{PI} as compared to homo-PI chains. The reason is as follows.

Equation 3 tells that in general the ϵ'' peak corresponds to a relaxation mode of the largest intensity g_p but does not always correspond to the slowest mode. For a broad mode distribution, the longest relaxation time τ_1 is generally much longer than the apparent τ_n. If the dielectric mode distributions (the distribution of τ_p and g_p; cf. eq 3) are not the same between the two systems under comparison, their ϵ'' peaks correspond to different modes and the comparison of nominal τ_n estimated from the loss maximum frequencies f_m (eq 4) does not make sense at all. As we have repeatedly emphasized,[1] comparison of τ_n makes sense and is identical to the comparison of the longest relaxation times τ_1 *only when* the systems to be compared have the same mode distribution and the ϵ'' curves of the same shape.

As seen in Figures 3–5, the PI/C14 solutions exhibit the relation $\epsilon'' \propto f$ at the low f side soon after the peak frequency f_m. This means that the slowest mode has the largest relaxation intensity (cf. eq 3) and τ_n is close to τ_1 for those PI/C14 solutions. On the other hand, SI bulk systems have a quite broad mode distribution that becomes narrower as C14 is added to decrease c_{SI}. The ϵ'' curves

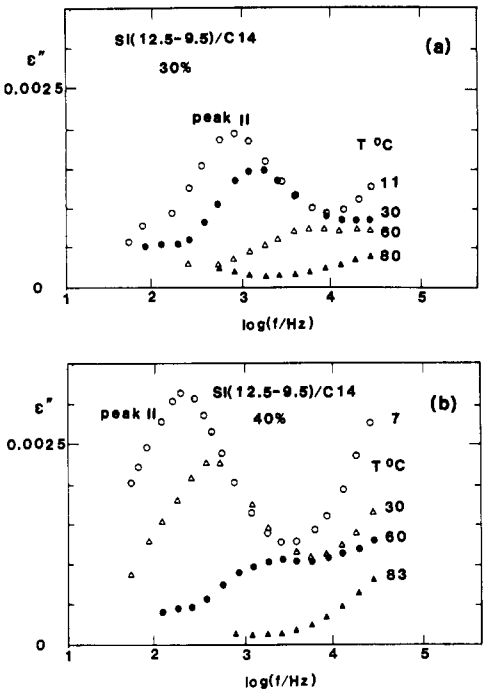

Figure 7. Dielectric loss curves at various temperatures for SI-(12.5–9.5)/C14 solutions with c_{SI} = (a) 30 and (b) 40 wt %. The peaks observed in this figure correspond to the peak II found in Figure 1.

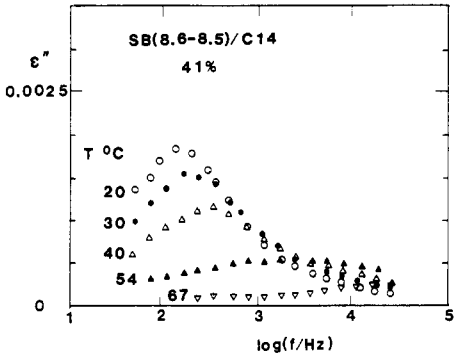

Figure 8. Dieletric loss curves at various temperatures for SB-(8.6–8.5)/C14 solutions with c_{SB} = 41 wt %. Note that the SB copolymer has no type-A dipoles and exhibits no dielectric normal-mode relaxation.

of the SI/C14 solutions exhibit only weak f dependence at the low f tail, indicating the terminal relaxation can be attained at much lower f. This broadening is the case even for the dilute SI(43–86)/C14 solution with c_{SI} = 2 wt % (cf. Figure 5). Thus the SI/C14 solutions should have τ_1 much longer than τ_n. It is likely that the τ_1 ($\gg\tau_n$) of the SI/C14 solutions are much longer than the τ_1 ($\cong\tau_n$) of the corresponding PI/C14 solutions.

IV-4. Domain relaxation: Now we turn our attention to the peak II relaxation shown in Figure 1. Parts a and b of Figure 7, respectively, show the ϵ'' curves of SI(12.5–9.5)/C14 with c_{SI} = 30 and 40 wt % at the temperatures as indicated. The peaks II are observed at low to intermediate f, and the increase in ϵ'' at the high f end is due to the normal-mode relaxation (peak I). Figure 8 shows similar ϵ'' curves of SB(8.6–8.5)/C14 solutions.

As seen in Figure 7, the peaks II of SI(12.5–9.5)/C14 solutions not only shift to the higher f side but also decrease their height with increasing T. Essentially the same behavior is found in Figure 8 for SB(8.6–8.5)/C14 solutions. The peak II is thus not due to the type-A dipoles of the I-blocks but is related to the PS microdomain structure commonly existing in the SI and SB/C14 solutions.

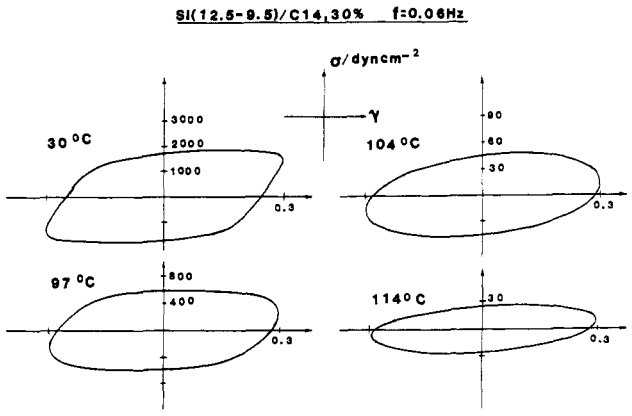

Figure 9. Comparison of stress–strain Lissajou's patterns at 0.06 Hz for a 30 wt % SI(12.5–9.5)/C14 solution at various temperatures as indicated. The strain amplitudes are 0.3 for all cases.

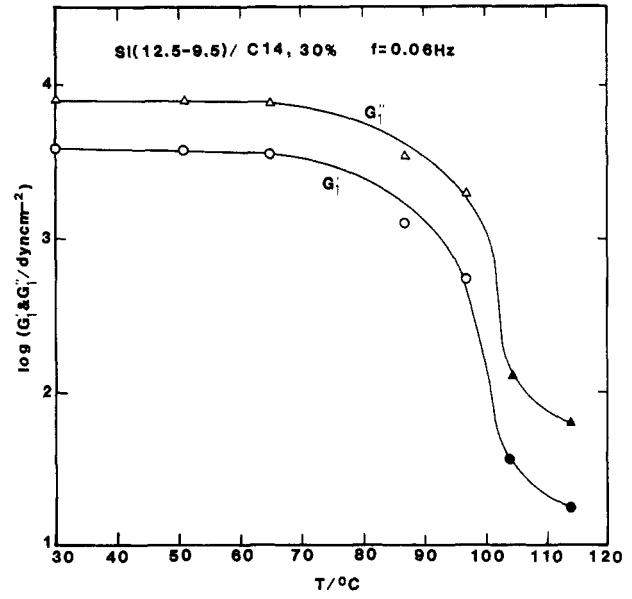

Figure 10. Temperature dependence of nonlinear moduli G_1' and G_1'' at 0.06 Hz for a 30 wt % SI(12.5–9.5)/C14 solution.

The decrease of the peak II height with increasing T may give a clue to elucidate the structure responsible to the peak II relaxation. From this point of view, we made rheological tests on SI(12.5–9.5)/C14 with c_{SI} = 30 wt % at various temperatures from 30 up to 114 °C. Figure 9 shows typical Lissajou's patterns of dynamic strain γ versus stress σ (f = 0.06 Hz) obtained at the temperatures indicated. We made Fourier analyses to evaluate the fundamental and higher order odd harmonics of the moduli, G_j' and G_j'' (j = 1, 3, ...) defined by a constitutive equation[12,17,18]

$$\gamma = \gamma_0 \sin \omega t, \quad \sigma = \gamma_0 \sum_{j=\text{odd}} [G_j' \sin j\omega t + G_j'' \cos j\omega t] \tag{6}$$

with γ_0 being the strain amplitude. Figure 10 shows the temperature dependence of the isochronal G_1' and G_1'' values at f = 0.06 Hz.

As seen in Figures 9 and 10, the solution at $T \leq 65$ °C exhibits a lozenge-shaped Lissajou's pattern characteristic of nonlinear viscoelastoplasticity, and the G_1' and G_1'' depend little on T. Although not shown here, the G_1' and G_1'' exhibited plateaus against f at $T \leq 65$ °C. All these results indicate the existence of a *stable* macrolattice at $T \leq 65$ °C.[12-18]

With further increase in T from 65 to 97 °C, the plateau levels of G_1' and G_1'' rather rapidly decrease. In this temperature range their f dependence also became significant. Weakening of the macrolattice must have been taking place in this temperature range. The solution, however, is still plastic even at 97 °C, exhibiting a lozenge-shaped Lissajou's pattern as seen in Figure 9. The result suggests the macrolattice is still preserved even at 97 °C.

Finally at high $T \geq 104$ °C, the solution becomes linear viscoelastic, exhibiting an elliptic Lissajou's pattern. The moduli decrease very rapidly with increasing $T \geq 104$ °C. Thus, in the SI(12.5–9.5)/C14 solution of c_{SI} = 30 wt %, the macrolattice disordering[12-18] took place at T between 97 and 104 °C. As judged from the changes in the rheological behavior of the SI(12.5–9.5)/C14 solution with c_{SI} = 30 wt % shown in Figures 9 and 10, the dielectric peak II relaxation visible in the SI/C14 as well as SB/C14 solutions from 11 to 60 °C is not attributable to the existence of the micelles themselves. The peak II almost disappears in both solutions at 80 °C, but the micelles are still preserved at $T \leq 97$ °C to form a macrolattice. Instead, the peak II is observable at $T < 65$ °C only when a stable macrolattice exists in the SI(12.5–9.5)/C14 as well as in the SB(8.6–8.5) solution.

A previous work[14] on SB/C14 solutions suggested that the mobility of SB junctions plays an important role on the stability of the macrolattice. From this point of view, it is interesting to note that the critical temperature (≅65 °C) at which the macrolattice becomes weakened and the peak II mode disappears in the SI(12.5–9.5)/C14 solution is fairly close to T_g^{PS} of swollen homo-PS of M_{PS} = 10.5 × 10^3 (and thus to T_g^{PS} of the S-domains of M_{PS} = 12.5 × 10^3 in the SI). However, it is not yet clear how such a stable macrolattice leads to the peak II mode and why the peak intensity almost vanishes before completion of the macrolattice disordering. Further study is necessary to solve these problems.

V. Conclusions

We found that the dielectric normal-mode relaxation of SI diblock copolymers is strongly affected by the addition of an I-selective solvent, *n*-tetradecane (C14), that reduces the spatial and thermodynamic confinements for the I-block chains tethered on the rigid S-cores, especially the latter, leading to the narrowing of the mode distribution. However, even in the micellar solution of very low c_{SI}, the dielectric behavior is still different from that of homo-PI molecules. This suggests that the thermodynamic confinement arising from densely populated neighboring I-block chains (tethered onto the S-cores) is still important even in the corona I-phase of an isolated micelle.

For SI/C14 solutions with intermediate c_{SI}, we found a new dielectric relaxation mode slower than the normal-mode relaxation. The new mode was observed also in similar SB/C14 micellar solutions. The changes in the rheological behavior of the solutions with temperature suggest that the new relaxation mode may be related to a stable macrolattice of micelles, which is common to both SI and SB systems, although at the moment we do not know how.

References and Notes

(1) Yao, M.-L.; Watanabe, H.; Adachi, K.; Kotaka, T. *Macromolecules* **1991**, *24*, 2955.
(2) Molau, G. E. In *Block Copolymers*; Agarwal, S. L., Ed.; Plenum Press: New York, 1970.
(3) See, for example: Holden, G. In *Block and Graft Copolymerization*; Cerasa, R. J., Ed.; Wiley: New York, 1973; Vol. 1.
(4) Meier, D. J. *J. Polym. Sci.* **1969**, *C26*, 81.

(5) Helfand, E.; Wasserman, Z. R. *Macromolecules* **1976**, *9*, 829; **1978**, *11*, 960.
(6) Leibler, L. *Macromolecules* **1980**, *13*, 1602.
(7) Stockmayer, W. H. *Pure Appl. Chem.* **1969**, *15*, 539.
(8) Adachi, K.; Kotaka, T. *Macromolecules* **1984**, *17*, 120.
(9) Adachi, K.; Kotaka, T. *Macromolecules* **1985**, *18*, 466.
(10) Imanishi, Y.; Adachi, K.; Kotaka, T. *J. Chem. Phys.* **1988**, *89*, 7585.
(11) Peyser, P. In *Polymer Handbook*, 3rd ed.; Brandrup, J., Immergut, E. H., Eds.; Wiley: New York, 1989.
(12) Watanabe, H.; Kotaka, T.; Hashimoto, T.; Shibayama, M.; Kawai, H. *J. Rheol.* **1982**, *26*, 153.
(13) Watanabe, H.; Kotaka, T. *J. Rheol.* **1983**, *27*, 223.
(14) Watanabe, H.; Kotaka, T. *Polym. J.* **1983**, *15*, 337.
(15) Shibayama, M.; Hashimoto, T.; Kawai, H. *Macromolecules* **1983**, *16*, 16.
(16) Hashimoto, T.; Shibayama, M.; Kawai, H.; Watanabe, H.; Kotaka, T. *Macromolecules* **1983**, *16*, 361.
(17) Watanabe, H.; Kotaka, T. *Polym. Eng. Rev.* **1984**, *4*, 73.
(18) Kotaka, T.; Watanabe, H. In *Current Topics in Polymer Science*; Ottenbrite, R. M., Utracki, L. A., Inoue, S., Eds.; Hanser Publishers: New York, 1987; Vol. II.
(19) Yoshida, H.; Watanabe, H.; Adachi, K.; Kotaka, T. *Macromolecules* **1991**, *24*, 2981.
(20) Graessley, W. W.; Edwards, S. F. *Polymer* **1981**, *22*, 1329.
(21) Sadron, C.; Gallot, B. *Macromol. Chem.* **1973**, *164*, 301.
(22) Yoshida, H.; Adachi, K.; Watanabe, H.; Kotaka, T. *Polym. J.* **1989**, *21*, 863.

Registry No. SI (copolymer), 105729-79-1; SB (copolymer), 106107-54-4.